



# Precipitation Detection Skill over Arbitrary Surfaces from AMSU-B/MHS

S. Joseph Munchak<sup>1,2</sup>, Benjamin Johnson<sup>1,3</sup>, Gail Skofronick-Jackson<sup>1</sup>

1: NASA Goddard Space Flight Center; 2: University of Maryland/ESSIC; 3: University of Maryland Baltimore County/ICET



## Motivation

Passive microwave remote sensing of frozen precipitation will be a key component of the Global Precipitation Measurement (GPM) mission. Compared to rain, additional difficulties are present in the form of high spatial and temporal variability of the surface emissivity over the high latitudes, as well as additional complexities in modeling the distribution and electromagnetic properties of frozen hydrometeors. Skofronick-Jackson et al. (2004), Noh et al. (2006), and Kim et al. (2008) establish the physical basis for using the channels surrounding the 183.3 GHz water vapor absorption line to mask the surface while still being sensitive to the scattering from ice particles in falling snow. This work demonstrates the skill of the channels available on the AMSU-B/MHS instruments in discriminating precipitation (as indicated by CloudSat) from non-precipitating scenes.

## Retrieval Method

Detection of precipitation with a radiometer fundamentally relies upon precipitation producing a unique radiometric signature that cannot be explained by realistic combinations of surface and atmospheric parameters. This can be formalized by defining a cost function:

$$\Phi = (y - f(\hat{x}))^T S_y^{-1} (y - f(\hat{x})) + (\hat{x} - x_a)^T S_a^{-1} (\hat{x} - x_a)$$

where a set of surface and non-precipitation atmospheric parameters ( $\mathbf{x}$ ) are adjusted so as to minimize the departure of simulated from observed brightness temperatures and the departure of the surface and atmospheric parameters from realistic values. This method is identical to that used by Bytheway and Kummerow (2010) to screen for precipitation over selected land surfaces with AMSR-E; in this study, we apply it to the AMSU-B and MHS sounding radiometers globally using CloudSat as a validation tool.

With only 5 channels, it is critical to carefully define  $\mathbf{x}$  and  $S_a$  so that they accurately represent the range of variability in the surface and atmosphere. We perform several experiments with different combinations of surface and atmospheric parameters listed in Table 1.

Parameter	Description	A priori value ( $x_a$ )	Variance ( $S_a$ )
Emissivity (1st component)	Ocean: Wind Land/Sea Ice: 1 <sup>st</sup> emissivity PC	Ocean: from AMSR-E Land/Sea Ice: 0	Ocean: 7.5 m/s Land/Sea Ice: 1 std. dev.
Emissivity (2nd component)	Ocean: SST Land/Sea Ice: 2 <sup>nd</sup> emissivity PC	Ocean: from AMSR-E Land/Sea Ice: 0	Ocean: 3 K Land/Sea Ice: 1 std. dev.
Water Vapor Profile	Mixing ratio at 14 standard pressure levels	ECMWF or AIRS	AIRS: Product uncertainty ECMWF: 25%
Cloud Water	1-km thick layer with base 1 km above surface	0.01 kg/m <sup>2</sup>	0.1 kg/m <sup>2</sup>

Table 1: Parameters used in retrieval experiments, along with their initial (a priori) value and variance.

## Emissivity Model

Over non-frozen ocean surfaces, we use the FASTEM4 model (Liu et al. 2011) which parameterizes emissivity as a function of frequency, angle, polarization, wind speed, and temperature. Over land and sea ice, we use a database of emissivity retrievals from AMSU-B and MHS under clear-sky conditions to create an empirical emissivity model for each 0.5° grid box for which at least 100 emissivity retrievals were available during 2007. The empirical model follows the formula:

$$E(f) = \mu(f) + \sigma(f) \sum_{i=1}^N \lambda_i(f) x_i$$

where  $\mu$  and  $\sigma$  are respectively the annual mean and stand deviation of emissivity and  $\lambda_i$  is the  $i^{\text{th}}$  empirical orthogonal function (EOF) of emissivity. The percent of 3-frequency variance explained by the 1<sup>st</sup> component is shown in Figure 1 and is quite high in most areas.

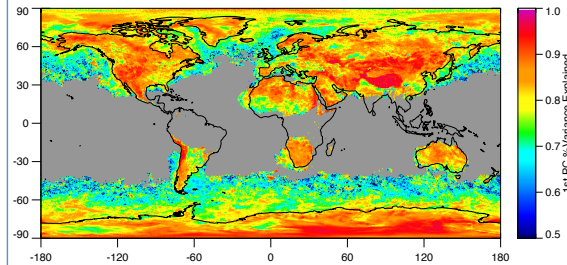


Figure 1: Percentage of 3-frequency (89, 150/157, and 183 GHz) emissivity variance explained by the 1<sup>st</sup> EOF of the empirical model. Note that no angular dependence is assumed. Gray indicates that <100 retrievals were available due to cloud cover or high water vapor content.

## Sample Retrieval

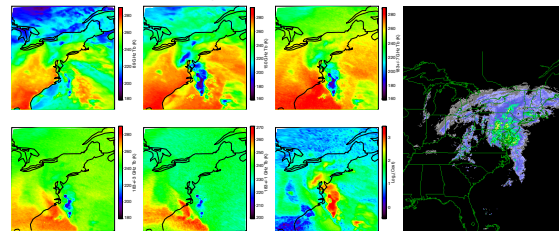


Figure 2: This case is from an East Coast snow/ice storm on February 14, 2007. The top three and bottom two panels on the left display the AMSU-B brightness temperatures, and the third bottom panel from the left shows the cost function value when only the first PC of surface emissivity (wind over ocean) is retrieved. High values correspond well to precipitation indicated by radar (courtesy UCAR) on the right panel, particularly values greater than 25 dBZ (indicated by green and yellow colors). Note the lack of artifacts related to coastlines or snow cover, which is present over much of the Great Lakes region at this time.

## Validation

One year (2007) of co-located CloudSat and AMSU-B/MHS data (courtesy Guosheng Liu of Florida State University) were processed with several versions of the retrieval, each using a different set of retrieval variables or ancillary data source (AIRS or ECMWF). For each AMSU-B/MHS pixel, the cost function ( $\Phi$ ) was minimized and stored in a database along with three CloudSat reflectivity metrics (maximum, surface, and mean) and ancillary surface classification information (primarily from AMSR-E).

The binary detection of precipitation requires two thresholds: A minimum value of  $\Phi$ , and a minimum value of CloudSat reflectivity ( $Z$ ), above which a pixel is considered to be precipitating for retrieval and validation purposes respectively. These thresholds can be optimized by maximizing the Heike Skill Score (HSS), which is a measure of the ability of the detection scheme to classify pixels correctly relative to random chance. HSS is defined as:

$$HSS = \frac{2(HC - FM)}{(H + F)(F + C) + (H + M)(M + C)}$$

$\Phi \geq \gamma$	$\Phi < \gamma$
$Z \geq x$ Hit (H)	Miss (M)
$Z < x$ False Alarm (F)	Correct Rejection (C)

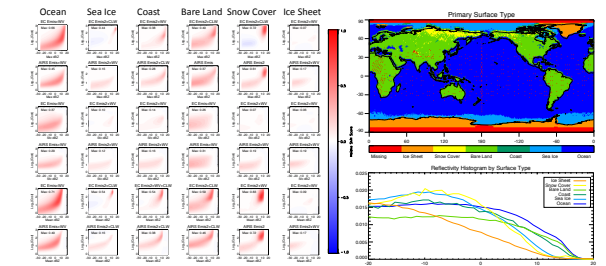


Figure 3: Left panels show HSS as a function of  $\Phi$  and  $Z$  for different surface types (columns) and different reflectivity metrics/ancillary data sources (rows). Only the best combination of parameters from Table 1 is shown (the parameters are indicated in the plot titles). To aid in interpretation, a map of the dominant surface type and reflectivity histograms for each surface type are shown on the right.

## Conclusions/Future Work

- Even with only 5 channels, AMSU-B/MHS are able to detect precipitation signal over many surface types using an optimal estimation-based retrieval of non-precipitating parameters.
- Worst skill is over sea ice and ice sheets, Surface complexity, lack of water vapor to mask the surface, or simply a lack of heavy precipitation events?
- Choice of ancillary dataset makes a difference (try climatology for first guess?)
- Over surfaces that work well, high correlation of mean/max reflectivity to  $\Phi$  indicates that this method can be used to quantitatively determine some column-integrated quantity of precipitation as well as detection.
- Best skill usually when retrieving two components of emissivity + water vapor.